Attenuation of Seismic Waves in the Trinidad & Tobago Area

Joan L. Latchman, William B. Ambeh and Lloyd Lynch
Seismic Research Unit, The University of the West Indies,
St. Augustine, Trinidad & Tobago, West Indies

Abstract

The attenuation of seismic waves from earthquakes located within the area bounded by 9-12 °N and 60-63 °W was estimated from short-period seismograms. Coda Q, Q_c, determinations were made for each of the six seismograph stations within the area, while spectral Q values from P-phases, Q_α were estimated for station TRN. The S-S single-scattering model was assumed for coda generation, and the ω^{-2} source model was assumed for the spectral Q determinations. The Q_c values show a strong frequency dependence in the frequency range 1.5 to 12 Hz. The value of Q at 1 Hz, Q_o, was found to lie within the range 107-132, while the rate of frequency dependence, n, extends from 0.80-1.06 for shallow events. For intermediate depth events, Q_o, varies from 101-173 and n from 0.80-1.02. The Q_α values obtained show a spatial variation within the region, with the highest attenuation being obtained on land Trinidad.

Introduction

Earthquake waves propagating through the earth lose amplitude. In seismology, loss of wave amplitude is termed attenuation, to which there are two contributing mechanisms - (a) intrinsic/anelastic attenuation and (b) apparent attenuation.

Intrinsic/anelastic attenuation results from actual loss mechanisms such as damped resonance, static hysteresis, relaxation and viscosity all of which are related to the 'internal friction' of the medium. Knopoff (1964), using terminology borrowed from electric circuit theory, defined attenuation by Q, the quality factor, such that:

$$Q^{-1} = (1/2\pi)\Delta W/W \qquad (1)$$

where W is the total amount of elastic energy stored per unit volume per cycle and ΔW is the part of W that is dissipated per cycle. Anelastic characteristics of solids are controlled by the thermal and defect properties, which are influenced by the thermal conductivity, grain size, defect concentration and mobility, diffusion rate and relatively weak interatomic and interdefect bonds at grain boundaries. Many of the mechanisms are activated processes that are strongly dependent on temperature and to a small extent on pressure (Jackson and Anderson, 1970).

Apparent attenuation may result from geometrical effects, such as refraction, reflection and scattering. Scattering of wave energy is believed to be caused by inhomogeneities comparable in scale to the wavelength of the elastic wave. This attenuation is linear and necessarily, highly frequency dependent. Although, in principle, this is a geometric mechanism, its mathematical form is similar to anelastic attenuation and therefore, cannot be removed from seismic amplitude data (Jackson and Anderson, 1970). Amplitudes of seismic body waves are also influenced by the velocity distribution in the medium. Arriving waves can travel along numerous travel paths such that some are strongly focussed or defocussed depending on the velocity structure (Der and McElfresh, 1976).

Local layering under the observing stations will also influence the spectra of body-wave arrivals (Der and McElfresh, 1976). If the soil conditions modify the incoming seismic waves in a simple and significant way, then we would expect that the same frequencies would always be amplified or deamplified irrespective of the earthquake source, mechanism or the direction from which seismic waves arrive. However, the effects due to geological discontinuities are strongly dependent on the 3-dimensional nature of soil deposits and on the direction of arriving waves. Therefore, the pattern of amplification caused by the local site conditions and transmission path has little chance of being repeated during any sequence of recorded earthquakes unless these would occur on the same fault and would have identical source mechanisms (Trifunac and Udwadia, 1974).

The construction of buildings with adequate earthquake resistance requires the estimation of the potential ground motion in future earthquakes. The effects observed at a given site are influenced by the attenuation of the region, the characteristics of the source and the local site conditions. Since the value of the attenuation parameter varies from region to region within the crust, in order to estimate the effects of an earthquake at any given distance from a specific source, it is important to have a measure of the absorption of the intervening area. The difference in felt area for earthquakes in the Western United States from comparable earthquakes in the Eastern United States, the former being larger than the latter, demonstrates the significance of differences in attenuation (Aki, 1982).

In this study, we estimate Q from microearthquakes in the Trinidad & Tobago area using two methods: the coda wave method (Aki and Chouet, 1975) and the spectral method (Al-Shukri et al., 1988).

Data Acquisition

The Seismic Research Unit network consists of a total of 30 stations. The sensor at each station is a single vertical component short-period 1 sec seismometer, which is either a Marks Product L4C or a Kinemerics Ranger SS1. The signal from each seismometer is amplified, fequency-modulated, then transmitted to the central recording site in St. Augustine, Trinidad, via VHF radio and/or microwave links. The signals are then demodulated, fed into PCs (15 stations per computer) and digitized by a 12 bit analogue to digital converter at 100 samples/sec. A triggering algorithm searches the resulting time series, from each station continuously, for possible earthquakes and stores the "event", preceded by a selectable length of pre-triggering time record, once preset triggering criteria are met.

Data, from each of the monitoring machines, are transferred to another PC, on which there is interactive software for picking phase arrival times and routine hypocentral determination. The network detects over 1500 events annually.

Methods

Coda Method

Coda waves, in this context, are the tail of a seismogram (after the arrival of major wave types such as P, S and surface waves) recorded at short distance from an earthquake. They have been explained by the back-scattering of waves by heterogeneities distributed in the large region outside the zone of the direct wave path from the source to the station. Whereas, it has been found that the spectral contents of the early part of a local earthquake seismogram depend strongly on the travel distance and the nature of the wave path to the station, the difference in spectrum among stations diminishes in the later part of the seismogram and disappears in the coda, a finding revealed by a common shape of coda amplitude decay curve (Aki and Chouet, 1975; Hermann, 1980).

In this study, we follow the techniques used by Ambeh and Lynch (1993). They made use of the single back scattering model of Aki and Chouet (1975), which assumes that the source and the receiver are coincident. This model gives the coda amplitude, A(flt) at frequency, f, and traveltime, t, as:

$$A(f|t) = C(f)t^{-\alpha}\exp(-\pi ft/Q_c) \quad (2)$$

where C(f) represents the coda source factor, α is a constant that depends on geometrical spreading and takes values of 1.0, 0.5 and 0.75 for body wave, surface wave and diffusion scattering respectively, and Q_c is the coda quality factor. Sato (1977) extended the model of Aki and Chouet (1975) to allow for source-receiver offset, which permits the coda analysis to begin immediately afer the shear wave arrival. For non-coincident source and receiver, the coda amplitude is given by:

$$A(r|t) = C(f)K(r,a)\exp(-\pi ft/Q_c) \quad (3)$$

where $a = t/t_s$, t_s is the S-wave lapse time, r is the source-receiver distance, $K(r,a) = (1/r)\{(1/a)\ln[(a+1)/(a-1)]\}^{0.5}$ and all the other symbols have the same meaning as in equation (2). Equation (4) is obtained by taking natural logarithms of equation (3) and rearranging terms:

$$\ln[A(r,f|t)/K(r,a)] = \ln C(f) - (\pi f/Q_c)t \quad (4)$$

For narrow bandpass filtered seismograms, C(f) is constant and hence by performing a linear regression of the term on the left-hand side of equation (4) with respect to t, Q_c can be found from the slope, which is the coefficient of t. If the S-S single scattering theory is correct, Q_c should equal Q_β, shear wave attenuation, determined directly from the S-wave, and indeed Aki (1980a, b) has found good agreement between them.

Spectral decay method

Displacement spectra can be derived from the seismograms of one or more instruments that span the body-wave band. Spectra are normally determined by Fourier transforming a waveform and smoothing the result. Source theories predict a constant long-period level, followed by a decay above a corner frequency that scales inversely with source size. A measure of seismic attenuation can be defined from the rate of high-frequency decay above the corner frequency (Cormier, 1982).

The instrument-corrected acceleration spectrum observed at a station, a distance r from the epicentre is defined by Anderson and Hough (1984) as:

$$A(r,f) = A_o \exp(-\pi ft^*) \quad (5)$$

such that

$$A_o = (2\pi f)^2 S(f)G(r,f) \quad (6)$$

where G(r, f) is the geometric spreading which if assumed to be independent of frequency, as in a homogeneous medium, is equal to 1/r for body waves, but which was not considered in this study and S(f) is the source displacement spectrum, which is often assumed to be proportional f^{-2} and is known as the ω^{-2} model (Brune, 1970). t^* is the attenuation time, and is given, for seismic phases by:

$$t^* = \int_{path} dr/QV \quad (7)$$

where Q is the attenuation quality factor, V is the seismic wave velocity and the integral is over the ray path. Now if Q is assumed constant over path then

$$t^* = t/Q \quad (8)$$

where t is the travel time. Substituting equation (8) in equation (5) and taking natural logarithms yields:

$$\ln A(f) = \ln A_o - \pi f t/Q \qquad (9)$$

which is the equation of a straight line having $\ln A_o$ as the intercept and $-\pi t/Q$ as gradient, from which Q can easily be determined (Al-Shukri et al., 1988).

Data

Coda-Q Analysis

The database of the Seismic Research Unit was searched for all events located within 9-12 °N and 60-63 °W for the period 1992/12/21 - 1993/06/30. The most recent data was used because reliable station calibrations are available from 1993/01/19. Such information being required for the spectral method for Q determination.

For coda-Q analysis, waveforms recorded at stations TCE, TRN, TPP, GRW, TBH and TPR were sought. Those with good signal to noise ratio, free of clipping and spikes were chosen. A total of 83 events met the criteria. The duration magnitudes of the events lie within the range 2.1 to 4.1 and their focal depths lie within 1 km to 124 km. Of the total number of events, each station had the following number of acceptable records: TCE - 70, TRN - 66, TPP - 26, GRW - 30, TBH - 39, TPR - 19 (Table 1).

Spectral Q analysis

Only TRN data were subjected to the spectral analysis method. Of the 54 events analyzed, 22 produced usable spectra. Their magnitudes lie in the range 2.2-3.4, focal depths from 3-108 km and epicentral distance from 33-169 km (Table 2).

Analysis

Coda method

Each seismogram time series was bandpass filtered over five frequency bands centred at 1.5, 3, 6, 12 and 24 Hz with bandwidths of 1, 2, 4, 8 and 16 Hz respectively, using an eight-pole, phase-free Butterworth filter. Starting at the S arrival, the root-mean-square (rms) amplitudes in each window were determined for the data in each frequency band, with the window sliding across the time series at 1 sec intervals. Time-window lengths for the rms averaging of 8 sec. (for centre frequencies of 1.5, 3 and 6 Hz) and 5 sec (for centre frequencies 12 and 24 Hz) were chosen so as to smooth out as much as possible irregularities in the amplitudes of the arrivals. The left-hand side of equation (4) was then evaluated and plotted against lapse time. From the plot, the linear portion, which had to be at least 25 sec long, was visually selected and a least squares straight line fitted to it. From the slope of the line, Q_c was calculated. The 25 sec window was chosen to allow the inclusion of many of the well-recorded smaller events. Q_c determination was restricted to the best linear portion to minimize the effect of small-scale, temporal variations in coda amplitude influenced by interference, secondary arrivals, or site conditions. Because of the generally poor quality of the results in the 24 Hz band, which may be due to the limited bandwidth of the instrument response, they were not included. Figure 1 shows the plots obtained for an event recorded by station TCE.

Spectral Method

A specified window of the P-phase was tapered using a cosine squared taper and Fourier transformed to produce a spectrum. Initially, various window lengths were tested. Although the spectra for window lengths of 0.6, 0.9, 1.2 and 1.5 seconds were produced, only that obtained from the 0.6 sec long window was used for this study because, like Al-Shukri et al. (1988), we found that the most favourable portion of the waveform from

Table 1: Parameters of events used in coda-*Q* analysis

YR MMDY	HRMN SEC	LAT	LONG	DEP	MAG	STATIONS
19921221	075129.83	10.9770N	62.0170W	97.24	3.1	TRN, GRW
19921222	044009.47	10.3460N	62.3100W	5.00	3.7	GRW
19921222	161311.96	11.4620N	62.0640W	124.27	3.4	TCE, TRN, TPP, TBH
19921227	094511.17	11.0250N	62.0940W	29.63	3.3	TCE, TPP, GRW
19921228	051433.03	10.6880N	61.6290W	5.00	2.8	TCE, TPP
19921228	100131.29	11.1100N	60.6400W	8.00	2.7	TRN
19921228	174531.51	11.2700N	62.1120W	100.35	3.2	TCE, TRN, GRW, TBH
19930106	182401.11	10.4140N	62.8590W	1.14	3.4	TCE, TRN, TPP, GRW
19930108	050012.95	10.9770N	61.1580W	10.00	2.1	TRN, TBH
19930108	124306.96	10.7570N	62.4350W	10.00	3.0	TCE, TRN, TPP
19930109	124407.02	10.5580N	61.3280W	32.96	2.5	TRN, TBH
19930109	194523.31	10.2640N	60.8390W	43.74	3.1	TRN, TPP, GRW
19930110	110920.55	11.1800N	60.9440W	1.51	3.2	TCE, TRN, TPP, GRW, TBH
19930110	134531.04	11.1350N	60.6020W	31.01	3.4	TCE
19930110	174153.99	11.1680N	61.8960W	64.81	2.5	TRN
19930110	201412.31	11.2100N	60.2230W	13.01	3.0	TCE, TRN
19930112	124648.09	10.5650N	61.6770W	15.06	2.6	TCE, TRN, TBH
19930112	193641.71	10.7440N	62.4940W	87.62	3.5	TCE, TRN, TBH
19930118	091356.21	10.3930N	62.2750W	10.00	3.5	TCE, TRN, TPP, GRW, TBH
19930119	080526.64	10.4410N	62.0290W	42.95	2.9	TCE, TRN, TPP, TBH
19930121	062449.43	10.5780N	61.3050W	5.00	3.1	TCE, TRN, TPP
19930121	104752.89	10.3790N	62.1740W	5.00	3.5	TCE, TRN, TPP, GRW, TBH
19930123	094436.63	10.3540N	61.3280W	50.80	2.2	TCE, TRN, TPP, TBH
19930124	002543.89	10.6690N	61.1060W	23.95	2.9	TCE, TRN
19930128	130730.39	11.2680N	60.4230W	33.21	3.4	TCE, TRN, GRW, TBH
19930214	050415.01	10.8120N	60.0040W	17.55	3.6	TCE, TRN, TPP, TBH
19930214	050925.25	10.9260N	60.0360W	24.45	3.3	TCE, TRN, TPP, GRW, TBH
19930214	123840.75	10.7120N	60.1520W	13.01	2.9	TCE, TRN, TBH, TPR
19930215	142053.83	9.7880N	62.4650W	33.00	3.2	TCE, TRN
19930215	204320.43	11.3430N	61.4860W	86.26	2.8	TCE, TRN, TBH
19930216	205828.56	10.2160N	60.1290W	82.34	3.4	TCE, GRW
19930218	053018.86	10.7590N	62.3670W	73.53	3.9	TCE, TPR
19930222	043638.86	10.8380N	62.3490W	86.80	3.0	TCE, TRN, GRW
19930222	071139.19	10.2500N	61.5510W	46.05	2.5	TCE, TRN, TPP
19930301	154023.49	10.8190N	62.1950W	73.04	3.0	TCE, TRN, GRW
19930302	124153.41	11.1100N	62.1220W	9.23	2.8	GRW
19930302	193045.72	11.1210N	62.1950W	8.40	2.9	TCE, TRN, GRW
19930304	235124.40	11.0990N	61.7490W	9.86	2.3	TCE, TRN
19930305	024650.92	11.2860N	61.7930W	10.10	2.5	TCE, TRN, GRW, TBH
19930305	093317.56	10.8910N	62.4000W	53.25	3.5	TCE, TRN TPP, GRW, TBH, TPR
19930308	071840.33	11.0770N	62.8860W	5.00	3.0	TCE, TRN
19930308	094845.12	10.9450N	61.5900W	21.21	2.9	TCE, TBH
19930308	103233.18	10.9100N	62.3130W	106.61	3.2	TCE, GRW, TBH, TPR
19930309	013459.14	10.8320N	62.1560W	23.21	3.0	TCE, TRN
19930311	192710.98	10.9670N	61.7570W	111.67	2.9	TCE, TRN
19930323	131142.30	11.1870N	61.7220W	43.76	3.0	TCE, TRN, GRW, TBH
19930329	101333.77	10.9480N	61.7580W	67.34	3.9	TPR
19930403	061734.73	11.0190N	62.1170W	73.89	3.1	TCE, TRN, GRW
19930404	040811.69	10.8790N	62.3970W	30.36	3.8	TCE, TPR
19930404	164046.41	11.0360N	61.9820W	111.91	3.5	TCE, TPP, TBH
19930404	181150.03	10.4710N	61.5350W	28.36	2.8	TCE, TRN
19930406	163808.85	10.0410N	61.1920W	48.99	3.5	TCE, TRN
19930411	130337.27	10.2590N	61.1970W	54.33	2.6	TCE, TRN, TPP, TBH
19930411	174900.47	11.1330N	62.5680W	3.00	3.3	TCE, TRN, TPP, TBH
19930415	123735.81	10.6480N	62.6520W	47.43	3.0	TCE, TRN
19930416	114314.14	11.3040N	61.2960W	14.80	3.2	TCE, TPP, TBH, TPR
19930416	225157.76	10.7890N	61.9540W	38.64	3.1	TCE, TRN, TPP
19930418	001452.50	10.7940N	62.4940W	67.20	3.0	TCE, TRN, TBH
19930418	021637.28	11.0580N	62.0100W	108.20	3.3	TCE, TRN, TBH, TPR
19930421	094559.15	11.1810N	62.8630W	6.17	3.2	TCE, TRN
19930422	093841.18	10.8440N	62.3740W	50.69	3.3	TCE, TRN, TPP
19930422	123157.15	10.5550N	62.4360W	108.58	4.1	TCE
19930426	120940.73	11.1160N	61.8390W	75.68	3.0	TCE, TRN
19930501	032311.57	10.9850N	60.0280W	19.32	2.7	TCE, TRN, TBH
19930505	234050.53	10.4320N	62.3100W	3.00	3.0	TCE, TRN
19930508	183813.91	11.1070N	62.2030W	111.99	3.9	TCE
19930512	094045.83	10.7490N	62.3970W	57.83	3.2	TCE, TRN
19930522	050314.80	10.7980N	62.5700W	3.00	3.3	TCE, TRN, TPP
19930522	102955.01	10.8670N	62.2340W	73.64	3.2	TPP, GRW, TBH
19930527	043731.32	11.5510N	61.0310W	24.31	2.9	TRN, GRW
19930529	001605.33	11.5880N	61.9790W	99.68	3.2	TCE, TRN, GRW, TBH
19930529	143203.56	11.1390N	61.6640W	48.08	3.0	TCE, TRN, GRW, TBH
19930531	075821.45	11.0800N	62.2370W	56.65	3.2	TCE, TRN, GRW, TBH
19930601	033431.80	10.8060N	62.4450W	52 17	3.1	TCE, TRN, TBH
19930601	124408.26	11.2390N	61.8380W	73.53	3.2	TCE, TRN, GRW, TBH
19930602	082203.77	11.3670N	62.2150W	106.94	3.2	TCE, TRN, TPP, GRW, TBH
19930603	164741.30	10.2060N	60.5500W	120 18	3.3	TCE, TRN, TBH
19930604	053953.88	11.3930N	62.0940W	73.59	3.1	TCE, TRN, GRW
19930604	115221.91	11.4630N	61.5180W	14 01	2.8	TRN GRW
19930605	180949 09	9.9650N	62.3460W	81 45	4 0	TCE, TRN, TBH
19930613	074815.69	10.2150N	62.3570W	3.00	3.6	TCE, TRN GRW, TBH
19930622	023514.87	11.9190N	61.7640W	111.88	3.2	TCE, TRN
19930623	122012.69	10.7070N	60.7900W	28.75	2.5	TBH

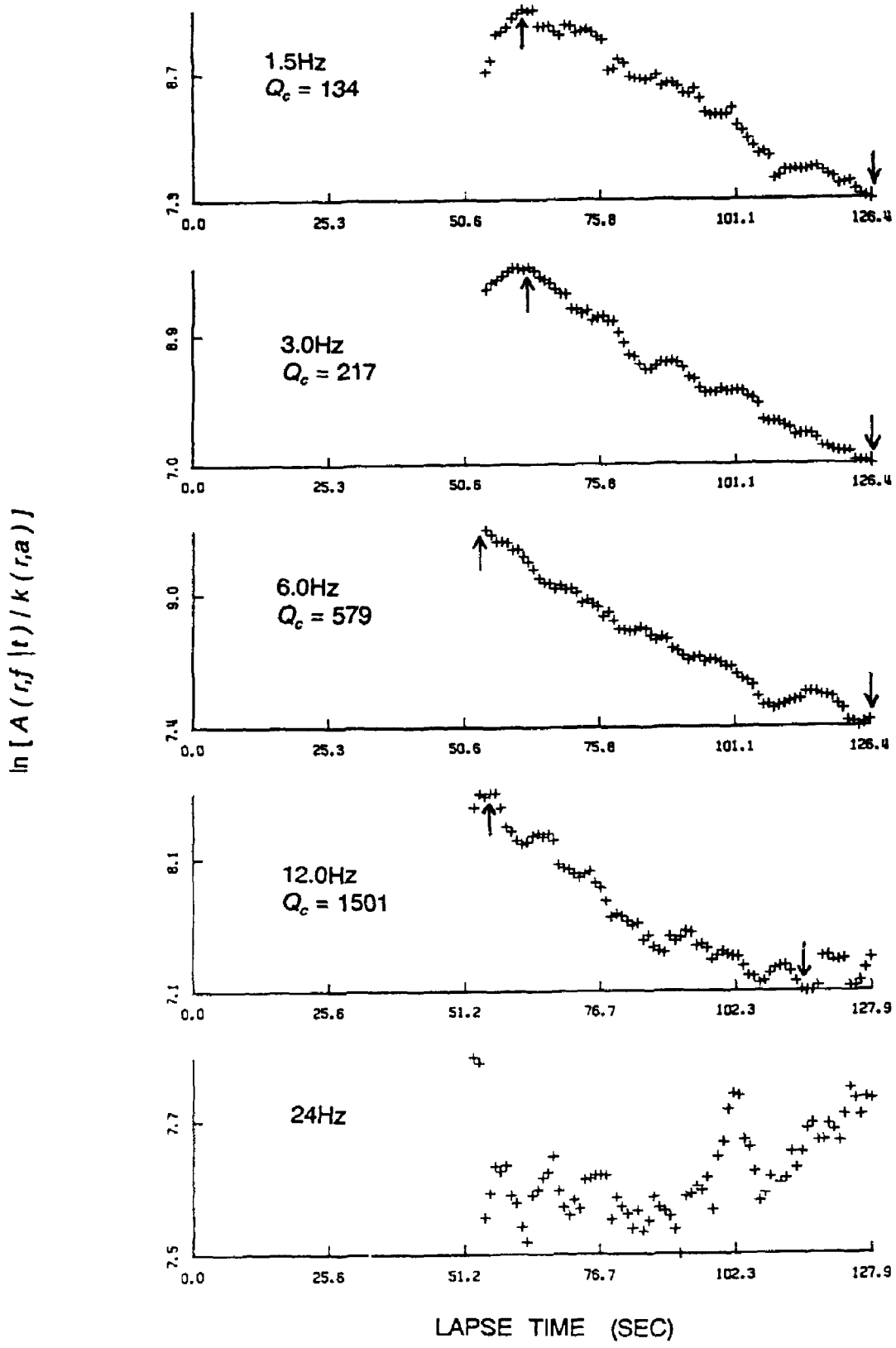

Figure 1: Example of coda-Q analysis as applied to station TCE seismogram for event of 1993/02/14 05 04 UTC The plot is for the quantity ln [$A(r, f \mid t) / k(r, a)$ versus Lapse Time, t The arrows indicate the portions chosen to determine Q_c

which to determine Q is its onset. In all cases, window lengths greater than 2.0 sec would include reflected/refracted phases and therefore,window lengths greater than 1.5 sec would not be useful. In many cases, this phenomenon was observed for window lengths greater than 0.6 sec. In all cases, the window began about 0.3 sec before the P-onset as given in the bulletin of the Seismic Research Unit. In one case, where there was a large P-residual, the window onset was revised. A noise sample, of length equal to that of the window, was taken 50 samples preceding the start of the window. This noise spectrum was removed from the P-phase spectrum and the resulting spectrum was smoothed five times.

The spectra were visually examined for portions at least 10 Hz long in which linear decay could be observed. There were five events with good spectra, for which decay occurred over 7.5 Hz. These were also included because of the clean spectrum shape. A least squares method was then used to fit a straight line to this portion of the spectrum. Q was determined from the gradient of the line by:

$$Q = TRAVT * \pi/GRAD \qquad (10)$$

where TRAVT is the travel time to the P-onset and GRAD is the gradient of the fitted line. An example of a spectrum obtained is shown in Figure 2.

Results

The results shown in Table 3 suggest that the average Q_c within the study area is relatively stable, for the given frequency bands, and does not vary significantly with depth. The ranges of Q_c for shallow events for the centre frequencies 1.5 Hz, 3.0 Hz, 6.0 Hz and 12.0 Hz respectively are 180-218, 213-315, 488-691 and 1141-1728 if the value of 2057 is not used since there is no intermediate depth value for the 12 Hz band for TPR. The ranges for intermediate depth events are 162-347, 250-354, 432-609 and 1106-1441. However, individual station results display some interesting differences. The results for TRN and TCE are, within error limits, the same except for the 1.5 Hz band, in which the value obtained for intermediate depth events recorded at TCE display somewhat reduced attenuation. This result was not observed by Ambeh and Lynch (1993) because of the very limited data for TCE and TRN in the intermediate depth range. Also, the figures obtained for TBH(S) in the 1.5-3.0 Hz range display slightly higher attenuation values.

Plots of Q_c values by frequency display a zonal variation of Q_c. This variation is more marked in the 3 Hz and 12 Hz bands. There is also a suggestion that the attenuation in east Trinidad is significantly different from that in west Trinidad. The plot for frequency band 3 Hz is shown in Figure 3.

Q_c variation with window length, average lapse time, epicentral distance, focal depth and magnitude

The results from stations TCE and TRN for frequencies 6 Hz and 12 Hz were examined for dependence on window length, average lapse time, epicentral distance, focal depth and magnitude. Figure 4 shows that there is no striking correlation between Q_c and any of these variables. However, the TRN results show a slight negative correlation between Q_c and focal depth and a slight positive correlation with average lapse time. This observation is at variance with the interpretation of Roecker et al. (1982) and Rovelli (1984) that increasing coda Q with increasing lapse time is due to increasing Q with depth.

Q_c variation and frequency dependence

Coda Q analysis in many regions has revealed a positive correlation between Q_c and frequency (e.g. Aki and Chouet, 1975; Rautian et al., 1978). The form of the dependence is generally given by:

$$Q_c = Q_o f^n \qquad (11)$$

Table 2: Parameters of events used in Spectral Analysis Method and related Q values

YR MMDY HRMN SEC	LAT	LONG	DEP	MAG	Q VALUES
19930123 094436 63	10 3540N	61 3280W	50 80	2 2	211 62 ± 8 79
19930128 130730 39	11 2680N	60.4230W	33 21	3 4	736 02 ± 55 48
19930214 050415 01	10 8120N	60 0040W	17 55	3 6	191 36 ± 3 22
19930214 123840.75	10 7120N	60 1520W	13 01	2 9	414 61 ± 17 19
19930222 071139 19	10.2500N	61 5510W	46 05	2 5	238.19 ± 5 45
19930302 124153 41	11 1100N	62 1220W	9 23	2 8	577 99 ± 15 61
19930304 235124 40	11.0990N	61 7490W	9 86	2.3	158 78 ± 3 42
19930305 024650 92	11.2860N	61 7930W	10 10	2.5	318 95 ± 5 01
19930308 071840.33	11.0770N	62 8860W	5 00	3 0	359.47 ± 18 69
19930323 131142.30	11 1870N	61 7220W	43.76	3 0	398.65 ± 5 63
19930403 061734.73	11.0190N	62.1170W	73 89	3 1	1080.73 ± 37 10
19930411 130337 27	10 2590N	61.1970W	54.33	2 6	278.28 ± 5 66
19930416 225157 76	10.7890N	61 9540W	38 64	3 1	150 71 ± 2.60
19930417 170619 39	10 3120N	62 2760W	3 00	3 4	352.57 ± 6 75
19930417 170742 99	10 2380N	62 1440W	3 00	3 3	195.42 ± 5 86
19930418 001452 50	10 7940N	62 4940W	67 20	3 0	240 01 ± 9 40
19930418 021637 28	11 0580N	62 0100W	108 20	3 3	509 61 ± 17 79
19930426 120940 73	11 1160N	61 8390W	75 68	3 0	512 68 ± 27 96
19930501 032311 57	10 9850N	60 0280W	19 32	2 7	669 80 ± 30 10
19930505 234050 53	10 4320N	62 3100W	3 00	3 0	364 40 ± 5 54
19930512 094045 83	10.7490N	62 3970W	57 83	3 2	443 58 ± 17 52
19930529 143203 56	11 1390N	61 6640W	48 08	3 0	302 47 ± 6.12

Table 3. Average Q_c values and their standard errors. Bracketed values are the number of Q used in the average. (S) indicates events less than 70 km deep, (I) indicates events greater than 70 km deep.

STATION	1.5Hz	3.0Hz	6.0Hz	12.0Hz
TCE(S)	184 ± 13 (27)	316 ± 16 (45)	636 ± 36 (43)	1193 ± 77 (27)
TCE(I)	347 ± 35 (11)	354 ± 18 (22)	609 ± 24 (23)	1262 ± 69 (16)
TRN(S)	218 ± 20 (32)	315 ± 21 (45)	563 ± 27 (47)	1160 ± 73 (36)
TRN(I)	216 ± 18 (11)	353 ± 25 (16)	564 ± 27 (18)	1106 ± 58 (17)
TPP(S)	211 ± 17 (15)	350 ± 22 (20)	613 ± 41 (13)	1141 ± 121 (1)
TPP(I)	183 ± 17 (1)	302 ± 19 (2)	586 ± 43 (3)	1454 ± 101 (1)
GRW(S)	176 ± 14 (9)	286 ± 15 (16)	488 ± 20 (15)	1728 ± 127 (13)
GRW(I)	136 ± 12 (3)	291 ± 15 (10)	544 ± 23 (12)	1441 ± 77 (10)
TBH(S)	180 ± 15 (10)	213 ± 11 (26)	539 ± 35 (19)	
TBH(I)	209 ± 23 (2)	250 ± 9 (13)	514 ± 25 (11)	
TPR(S)	205 ± 21 (4)	292 ± 15 (5)	691 ± 52 (6)	2057 ± 200 (4)
TPR(I)	162 ± 9 (1)	305 ± 26 (2)	432 ± 19 (3)	

Table 4 Q_0 obtained for shallow, intermediate and all events using the relationship $Q_c = Q_0 f^n$

STAT	SHALLOW EVENTS		INTERMEDIATE EVENTS		ALL EVENTS	
	Q_0	n	Q_0	n	Q_0	n
TCE	116	0 89±0 04	173	0 74±0 07	131	0 85±0 04
TRN	132	0 80±0 04	136	0 80±0 06	133	0 80±0 04
TPR	107	1 06±0 13	101	0 92±0 16	105	1 02±0 11

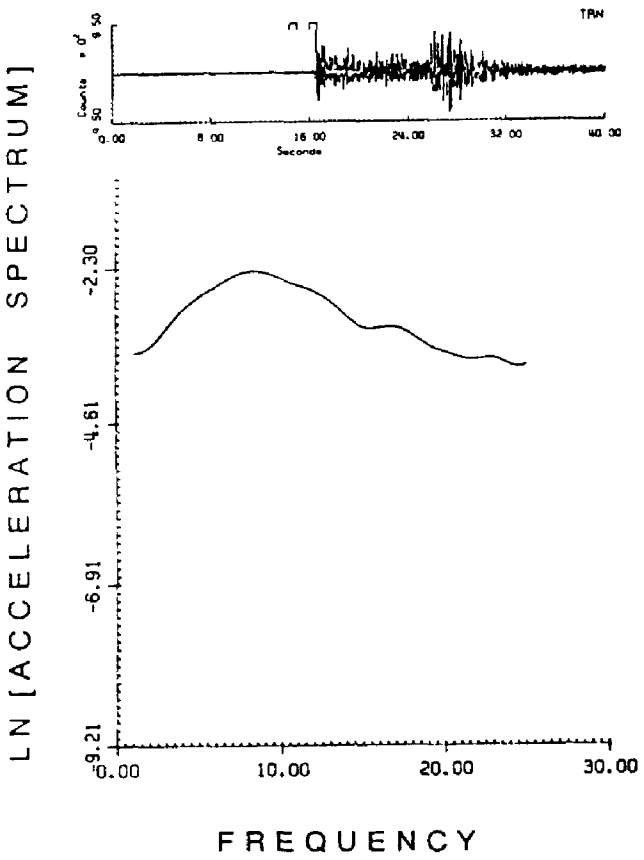

Figure 2: Example of spectral-Q analysis for an event 68 km from station TRN on 1993/03/23 at 13:11 UTC located at 11.2°N 61.7°W 44 km Mt = 3.0. The plot is for Ln (Acceleration Spectrum) versus Frequency

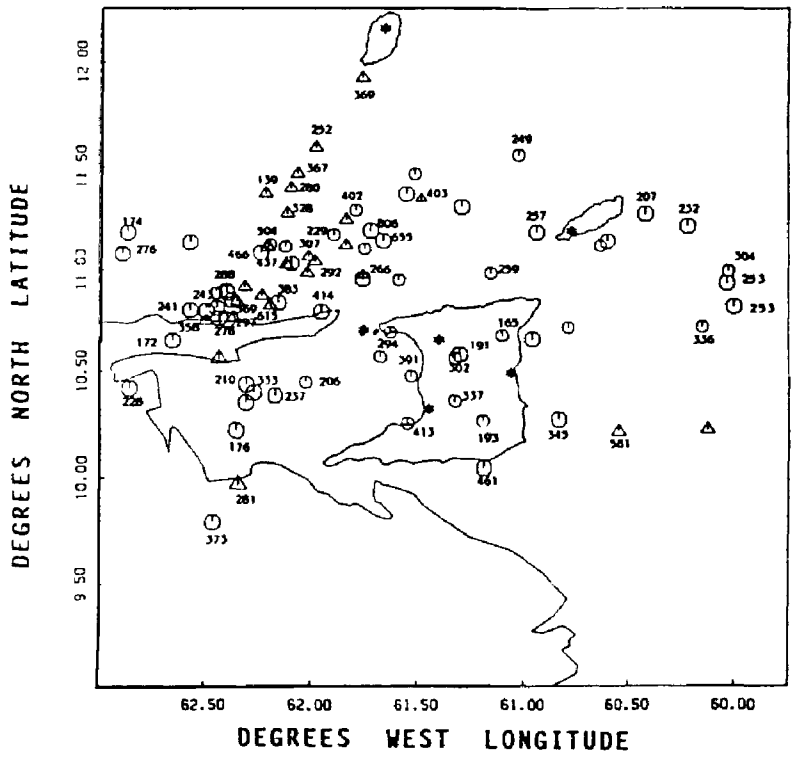

Figure 3: Q_c values for events recorded at TRN, frequency band 3.0 Hz.

where n has been found to lie mainly in the range 0.5 to 1.1. The Q_c values of this study were fitted to the above equation. The results are given in Table 4.

The results obtained in each frequency band were not uniformly abundant. For individual stations the band with disproportionate numbers of results were excluded. The usable bands obained for each station are as follows: TCE - 1.5, 3.0, 6.0, 12.0; TRN - 1.5, 3.0, 6.0, 12.0; TPP - 1.5, 3.0, 6.0; GRW - 3.0, 6.0, 12.0; TBH - 3.0, 6.0; TPR - 1.5, 3.0, 6.0, 12.0. Only those stations with data in all four bands are here displayed.

Spectral Q for TRN

The results from the limited data used in this study indicate a spatial variation of the attenuation parameter. In general, the highest attenuation is observed on land Trinidad (Figure 3).

Discussion and Conclusions

Of the 83 events used in the coda Q analysis, 25 were of intermediate depth (≈30%) and of the 22 with usable P-wave spectra, there were 3 events (≈14%) of intermediate depth.

The average Q_α for the shallow events is 348 and 701 for the intermediate depth events. 348 compares very well with the Frankel (1982) value of 380 found using arrivals to three stations in the northeastern Caribbean, for frequencies 5-20 Hz. His data set consisted of events less than 50 km in depth. The values of Q_c for TRN (see Table 2) are 218, 315, 563 and 1160 for shallow events at 1.5, 3.0, 6.0 and 12 Hz respectively and 216, 353, 564 and 1106 for intermediate depth events. Frankel's (1982) average from two stations for Q_β is 400. In the determination of Q_α, decay was usually observed above 5 Hz. Therefore, a comparison of Q_β and Q_α made in the 6 and 12 Hz bands and using the average of 862 for Q_β reveals that P-wave attenuation is greater than S-wave attenuation such that $Q_\alpha \approx 0.40 Q_\beta$. However, our observations suggest that simply averaging Q_α and Q_c for all the results may be misleading.

In the S-S single scattering model, the scatterers responsible for the generation of coda waves are located on the surface of an ellipsoid whose surface projection is defined by the equation:

$$x^2/(vt/2)^2 + y^2/[(vt/2)^2 - R^2/4] = 1 \qquad (12)$$

for a surface source. Here R is the source-receiver distance, v is the velocity, t is the lapse time and x and y are the surface coordinates (Pulli, 1984). In the study area, Q_c estimates at an average lapse time of 52 sec correspond to sampling volumes about 208 km in lateral extent, 137 km in depth and 16,500 km^2 in surface area (Ambeh and Lynch, 1993). Therefore, waves arriving at any station within the study area should have sampled largely overlapping volumes. A zonal variation in the Q_c values obtained should not be apparent. However, our results suggest that such a variation exists. This is not conclusive because an investigation of zonal variation of Q_c was not one of the original objectives of this study and the techniques employed were not tailored to cater to it. The Q_α results prompted the Q_c plots. A future study would need to be done, restricting the lapse time to a constant value and so restricting the sampled volume to a fixed size. It should be noted that because 25 sec was the minimum lapse time used, the extent of the ellipsoid for some events was as small as 100 km ad 88 km in depth and, therefore, those events onland Trinidad for example could have a sampled ellipsoid composed largely of on land scatterers.

Clearly, a sampled surface as symmetrical as an ellipsoid must assume a uniform distribution of heterogeneities (Aki, 1969). Although this may be a valid assumption for a tectonically stable region such as the Central United States (Pulli and Aki, 1981), it is probably not applicable in an area as tectonically complex as the study area. It might be that

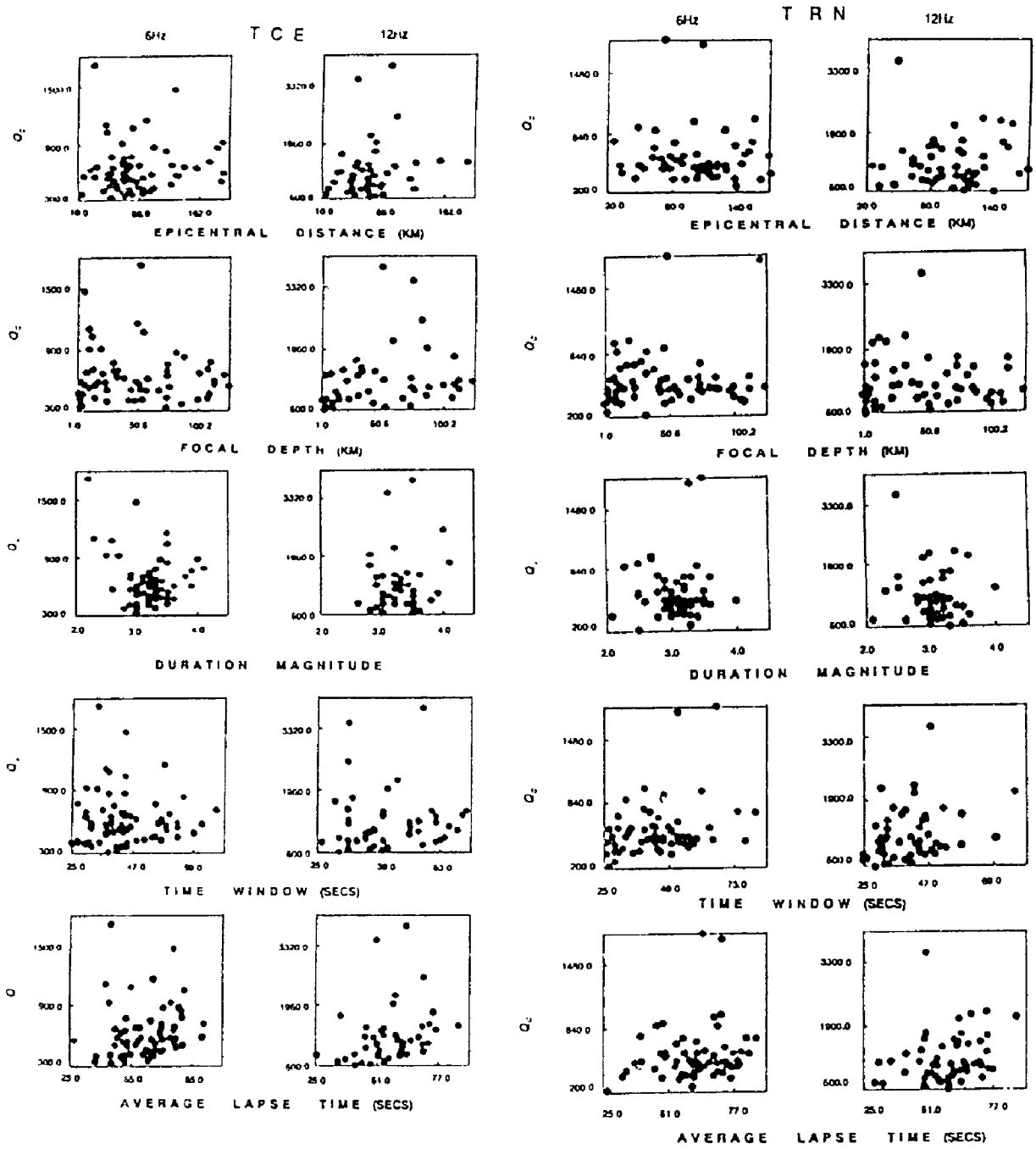

Figure 4: Variation of Q_c with window length, average lapse time, epicentral distance, focal depth and magnitude.

the complex nature of the area reduces the expected overlap thus allowing genuine zonal variations to be revealed. The observation by Sutton et al. (1967) that attenuation appears to be affected by the orientation of the structural trend with respect to event location may also contribute to the observed differences in attenuation.

Differences in attenuation at different frequencies observed at populated sites have important implications with regard to hazard/risk and should not be casually treated. The lessons learned from the Michoacan, Mexico, earthquake of 1985 forcefully demonstrate the potential for great disaster when various influences combine in time and place e.g. the occurrence of an earthquake rich in 2 sec energy, the efficient propagation of that energy to Mexico City and a site capable of greatly amplifying 2 sec energy (Singh et al., 1988).

In the determination of Q_α geometric spreading was not taken into account and indeed the Q_α values obtained must incorporate this effect. Also, it was assumed that Q is constant over the travel path, which allowed equation (7) to be used. The results, however, indicate that Q does vary over the path and, therefore, the use of equation (7) is not strictly accurate.

References

Aki, K. (1969). Analysis of seismic coda of local earthquakes as scattered waves. J. Geophys. Res., 74: 615-631.

Aki, K. (1980a). Attenuation of shear waves in the lithosphere for frequency from 0.05 to 25 Hz. Phys. Earth Planet. Inter., 21: 50-60.

Aki, K. (1980b). Scattering and attenuation of shear waves in the lithosphere. J. Geophys. Res., 85: 6496-6504.

Aki, K. (1982). Scattering and Attenuation. Bull. Seism. Soc. Am., 72: S319-S330.

Aki, K. and Chouet, B. (1975). Origin of coda waves: source, attenuation and scattering effects. J. Geophys. Res., 80: 3322-3342.

Al-Shukri, H., Mitchell, B.J. and Ghalib, H.A. (1988). Attenuation of seismic waves in the New Madrid seismic zone. Seism. Res. lett., 59: 133-140.

Ambeh, W.B. and Lynch, L. (1993). Coda Q in the eastern Caribbean, West Indies. Geophys. J. Int., 112: 507-516.

Anderson, J.G. and Hough, S.E. (1984). A model for the shape of the fourier amplitude spectrum of acceleration at high frequencies. Bull. Seism. Soc. Am., 74: 1969-1993.

Cormier, V.F. (1982). The effect of attenuation on seismic body waves. Bull Seism. Soc. Am., 72: S169-S200.

Der, Z.A. and McElfresh, T.W. (1976). Short-period P-wave attenuation along various paths in North America as determined from P-wave spectra of the SALMON nuclear explosion. Bull. Seism. Soc. Am., 66: 1609-1623.

Frankel, A. (1982). The effects of attenuation and site response on the spectra of microearthquakes in the northeastern Caribbean. Bull. Seism. Soc. Am., 72: 1379-1402.

Herrmann, R.B. (1980). Q estimates using the coda of local earthquakes. Bull. Seism. Soc. Am., 70: 447-468.

Jackson, D.D. and Anderson, D.L. (1970). Physical mechanisms of seismic wave attenuation. Rev. Geophys. Space Phys., 8: 1-63.

Knopoff, L. (1964). Q. Rev. Geophys., 2: 625-660.

Pulli, J.J. (1984). Attenuation of coda waves in New England. Bull. Seism. Soc. Am., 74: 1149-1166.

Pulli, J.J. and Aki, K. (1981). Attenuation of seismic waves in the lithosphere: comparison of active and stable areas. In: Beavers, J.E. (ed.). Earthquakes and Earthquake Engineering: The Eastern United States. Ann Arbor Science Publishers Inc., Ann Arbor, pp. 121-141.

Rautian, T.G., Khalturin, V.I., Martinov, V.G. and Molnar, P. (1978). Preliminary analysis of the spectral content of P- and S-waves from local earthquakes in the Garm, Tadjikistan region. Bull. Seism. Soc. Am., 68: 948-971.

Rebollar, C.J., Traslosheros, C. and Alvarez, R. (1985). Estimates of seismic wave attenuation in northern Baja California. Bull. Seism. Soc. Am., 75: 1371-1382.

Reiter, L. (1990). Earthquake Hazard Analysis: issues and insights. Columbia University Press, New York.

Roecker, S.W., Tucker, B., King, J. and Hatzfeld, D. (1982). Estimates of Q in Central Asia as a function of frequency and depth using the coda of locally recorded earthquakes. Bull. Seism. Soc. Am., 72: 129-149.

Rovelli, A. (1984). Seismic Q for the lithosphere of the Montenegro region (Yugolsavia): frequency, depth and time windowing effects. Phys. Earth Planet. Inter., 4: 159-172.

Sato, H. (1977). Energy propagation including scattering effects. Single isotropic scattering approximation. J. Phys. Earth, 24: 27-41.

Singh, S.K., Lenmo, J., Dominguez, T., Ordaz, M., Espinosa, J.M., Mena, E. and Quaas, R. (1988). The Mexico earthquake of September 19, 1985 - A study of amplification of seismic waves in the valley of Mexico with respect to a hill zone site. Earthquake Spectra, 4: 653-673.

Sutton, G.H., Mitronovas, W. and Pomeroy, P.W. (1967). Short-period seismic energy radiation patterns from underground nuclear explosions and small-magnitude earthquakes. Bull. Seism. Soc. Am., 57: 249-268.